



***In Situ* Observations and Pressure Measurements for Autoclave Co-Cure of Honeycomb Core Sandwich Structures**

Mark Anders*, Daniel Zebrine, Timotei Centea, and Steven Nutt

M.C. Gill Composites Center, Viterbi School of Engineering, University of Southern California,
3651 Watt Way, VHE-708, Los Angeles, California, 90089, United States.

*Corresponding author's e-mail: anders@usc.edu

Abstract:

In this article, we describe an experimental method for investigating the autoclave co-cure of honeycomb core composite sandwich structures. The design and capabilities of a custom-built, lab-scale “*in situ* co-cure fixture” are presented, including procedures and representative results for three types of experiments. The first type of experiment involves measuring changes in gas pressure on either side of a prepreg laminate to determine the prepreg air permeability. The second type involves co-curing composite samples using regulated, constant pressures, to study material behaviors in controlled conditions. For the final type, “realistic” co-cure, samples are processed in conditions mimicking autoclave cure, where the gas pressure in the honeycomb core evolves naturally due to the competing effects of air evacuation and moisture desorption from the core cell walls. The in-situ co-cure fixture contains temperature and pressure sensors, and derives its name from a glass window that enables direct in-situ visual observation of the skin/core bond-line during processing, shedding light on physical phenomena that are not observable in a traditional manufacturing setting. The experiments presented here are a first step within a larger research effort, whose long-term goal is to develop a physics-based process model for autoclave co-cure.



1. INTRODUCTION

The aerospace composites industry has grown tremendously in recent decades, and is predicted to continue expanding rapidly for the foreseeable future. Due to demand exceeding production capacity in many sectors, there exists a critical and ongoing need for improved manufacturing practices, which today often rely on trial-and-error solutions to problems encountered during production. This work offers an approach to troubleshooting and optimizing autoclave co-cure of honeycomb core sandwich structures using *in situ* process diagnostics. By mimicking autoclave co-cure at the lab-scale with a highly-instrumented tool that contains a glass viewport, we shed light on real-time behavior of physical phenomena that are not observable in standard manufacturing settings.

Composite sandwich structures are constructed from a low-density honeycomb core bonded with a film adhesive to two fiber-reinforced laminated face-sheets (skins) [1]. Under bending loads, the skins carry most of the tensile or compressive stresses, while the core transfers shear loads between them. These structures are widely used in aerospace and other weight-critical applications because distancing the skins from the neutral bending axis dramatically increases the specific flexural stiffness and strength compared to monolithic laminates (analogous to an I-beam versus a rectangular beam). Face-sheets typically consist of several plies of prepreg (carbon or glass fabric pre-impregnated with uncured thermoset resin), which can be cured by traditional autoclave or out-of-autoclave (VBO: Vacuum Bag Only) methods and then secondarily bonded to the core. This relatively straightforward procedure can produce high-quality sandwich structures. However, the preferred manufacturing technique is co-cure, in which the skins are simultaneously cured and bonded to the core. Although co-cure has the advantage of being a single-step process, it introduces significant additional complexity due to the interactions of many coupled physical phenomena,

Please cite this article as: Mark Anders, Daniel Zebrine, Timotei Centea, and Steven Nutt, “*In Situ Observations and Pressure Measurements for Autoclave Co-Cure of Honeycomb Core Sandwich Structures*”, Journal of Manufacturing Science and Engineering, 139(11), 111012 (2017). DOI: 10.1115/1.4037432



including consolidation of the face-sheets, flow of the film adhesive, and evolution of the gas pressure in the core due to air evacuation and moisture vaporization. Complications arise due to coupling of these effects: prepreg resin can bleed into the core, film adhesive can infiltrate the prepreg, gasses in the core must be evacuated through the skins, and sub-ambient core pressures can cause adhesive foaming and void formation.

Campbell [1] has described how autoclave co-cure is possible yet challenging, since the pressure required to suppress porosity in the face-sheets can result in face-sheet dimpling or pillowing when cured against a honeycomb core, as well as core crushing and core migration. Grove et al. [2] conducted an experimental study relating processing parameters to the strength of the skin/core bond in out-of-autoclave co-cure, showing that the cure temperature is a dominant parameter and that heating ramp rate, vacuum quality, and time of vacuum application also have non-negligible effects. Tavares et al. conducted a series of studies [3–7] analyzing the influence of prepreg air permeability on the core pressure during processing. They showed that the gas pressure within the core can influence fillet geometry, skin-to-core distance, and adhesion strength, and that an optimal range of core pressures exists. They investigated the behavior of fully-impregnated prepreg and partially impregnated “semipreg” (with a much higher out-of-plane permeability), which enabled enhanced core evacuation but was also prone to exhibiting resin bleed into the core. They demonstrated the successful manufacturing of thick-skinned sandwich structures using hybrid laminates containing both types of prepreg. Kratz and Hubert [8–11] conducted a similar study, relating material properties, air permeability, and the resultant magnitude, rate, and consistency of air evacuation from the core. They developed a predictive model for core pressure and showed agreement with *in situ* core pressure measurements. They also considered the anisotropy of prepreg air permeability, which can lead to in-plane core pressure variations when scaling-up to larger parts.



Tavares et al. and Kratz et al. both utilized lab-scale co-cure fixtures, which consisted of a tool plate with a recessed pocket into which honeycomb core was placed and then covered with prepreg, forming a “half-sandwich” assembly with only one skin. Core pressure was measured using a pressure sensor mounted into the pocket. However, both tools considered only VBO processing, in which the tool was placed into an oven, limiting compaction pressure to only one atmosphere. Furthermore, all of the aforementioned papers considered post-mortem quality analysis only (e.g. microscopy of cut and polished sections), resulting in information pertaining to the final state of the cured parts, but no information about microstructural changes during processing. This work, in contrast, describes the design and capabilities of an “*in situ* co-cure fixture” (see Figure 1 and Figure 2), which enables core pressure measurements at elevated autoclave pressures, and provides real-time information about the skin/core bond-line evolution.

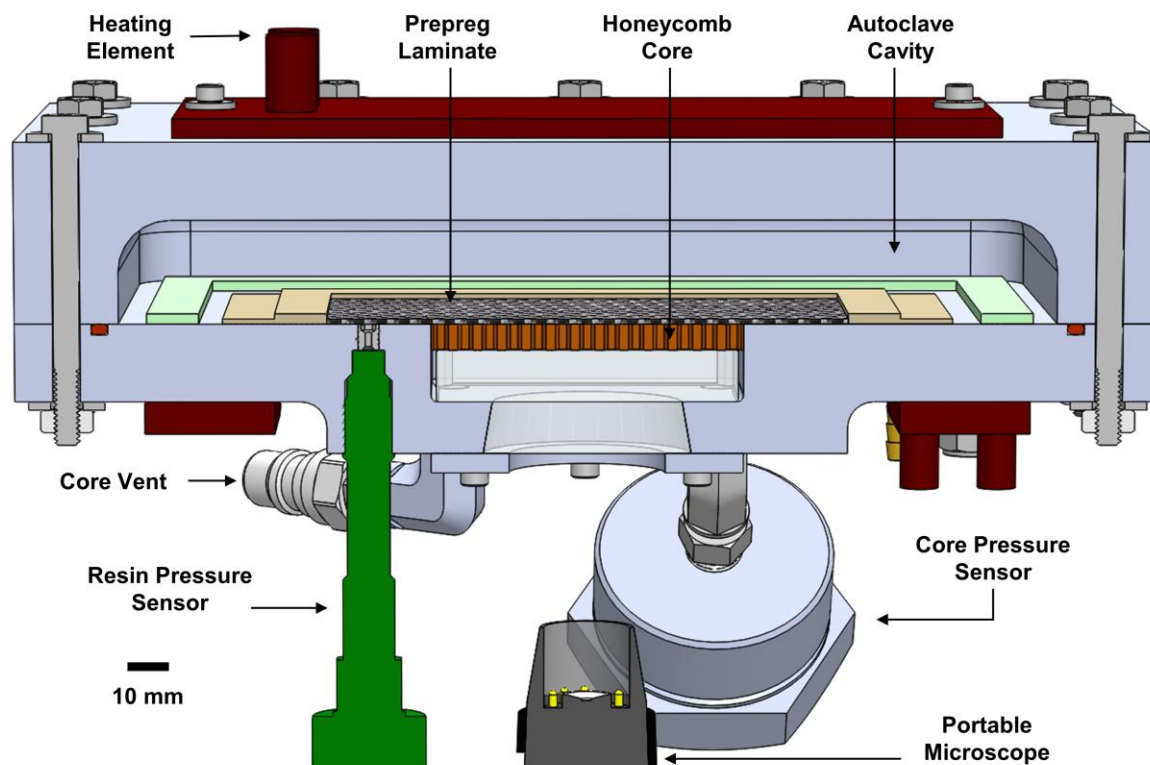


Figure 1: Section view from a CAD model of the “*in situ* co-cure fixture”

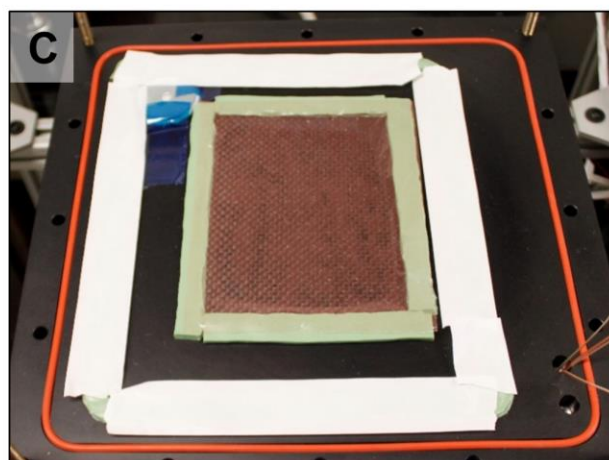
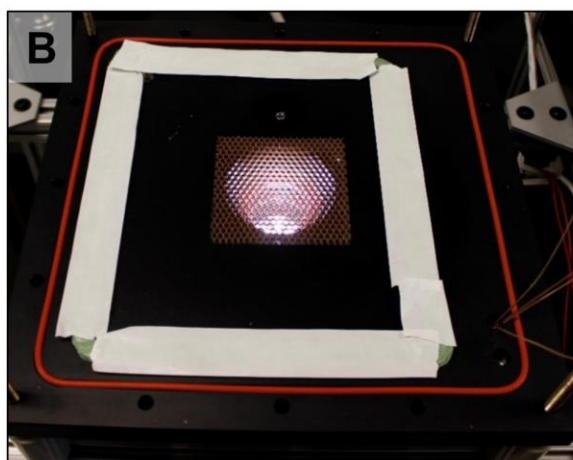
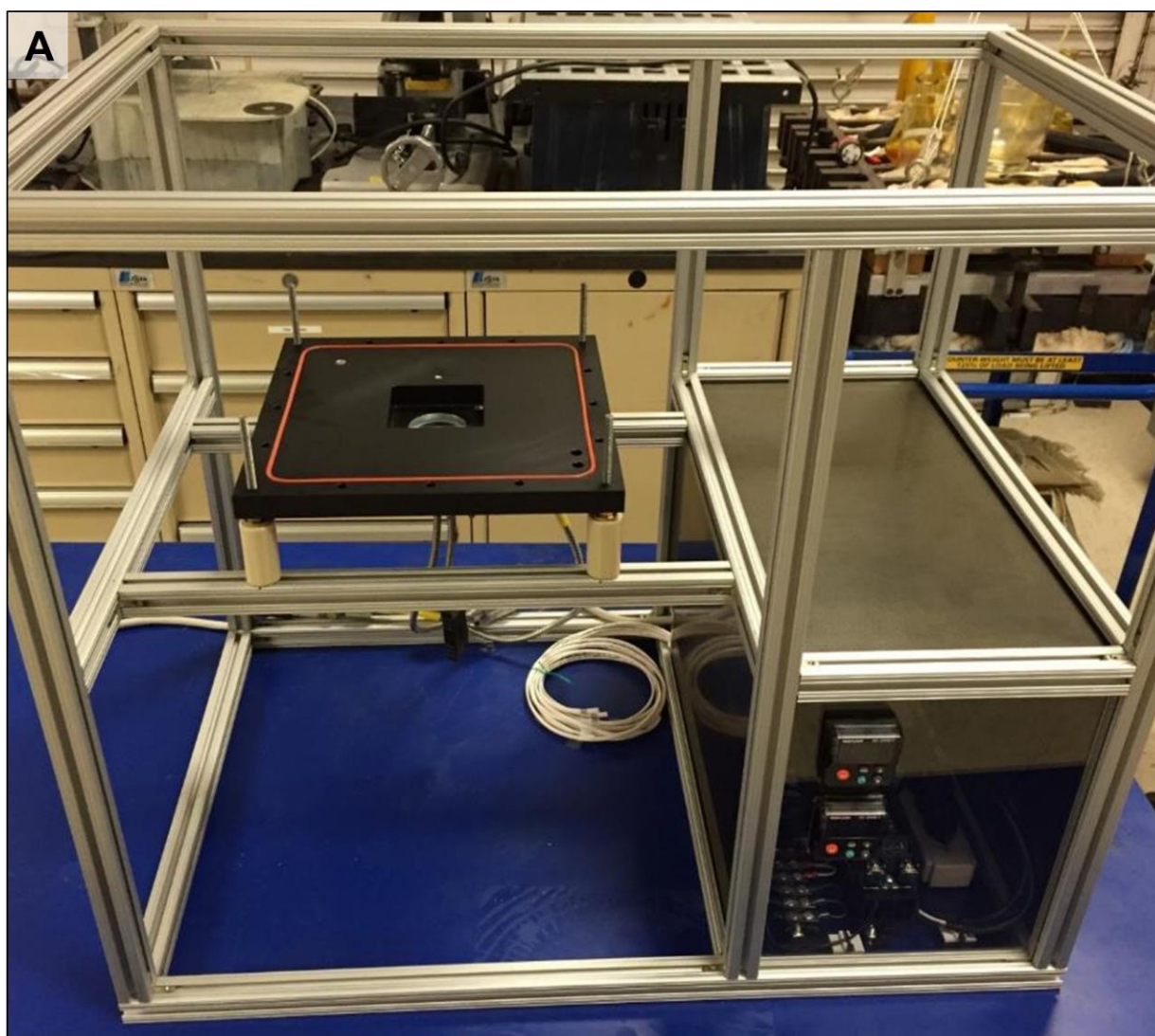


Figure 2: Photographs of the in situ co-cure fixture. (a) Tool plate with core pocket visible, mounted to frame, without lid. (b) Honeycomb core in the pocket, with tape for the vacuum bag around the edges. (c) Tool plate with laminate placed over core.

Please cite this article as: Mark Anders, Daniel Zebrine, Timotei Centea, and Steven Nutt, “*In Situ Observations and Pressure Measurements for Autoclave Co-Cure of Honeycomb Core Sandwich Structures*”, Journal of Manufacturing Science and Engineering, 139(11), 111012 (2017). DOI: 10.1115/1.4037432



The overall goal of our research is to develop fundamental understanding of the physical phenomena relevant to autoclave co-cure – particularly as related to defect/void formation – and then leverage that understanding to develop optimized procedures for reliable, robust, and efficient composite fabrication. A first step towards achieving this goal was to design and build a tool to enable *in situ* process characterization, which is the topic of this paper. Ongoing experiments with this tool will ultimately be used to develop and validate a physics-based process model for autoclave co-cure of sandwich structures.

2. MATERIALS

Two prepreg systems were used for this study. The first was HexPly AGP193PW/8552S (193 g/m² fiber areal weight, plain weave, AS4 fibers, 3000 fibers/tow, 38% resin content, Hexcel Corp.), a common fully-impregnated aerospace carbon/epoxy prepreg designed for autoclave processing. The second was a newer carbon/epoxy prepreg: Cycom 5320-1 (plain weave, T650 fibers, 3000 fibers/tow, Cytec Solvay), with a partially-impregnated microstructure designed to enhance air evacuation for VBO processing. The film adhesive was also an epoxy: Loctite EA 9658 AERO (290 g/m² unsupported film, Henkel Aerospace Materials), which contains aluminum powder as a toughening agent. The core material was HD132 (Gill Corp.): 3.2 mm hexagonal cells of phenolic-dipped aramid (Nomex) paper, 12.7 mm thick, with a density of 48 kg/m³ (3 lb/ft³).

3. *IN SITU* CO-CURE FIXTURE: DESIGN

A schematic section view of the *in situ* co-cure fixture is shown in Figure 1. The main body of the fixture is an anodized aluminum tool plate, 280 mm square and 19 mm thick. The center of the plate contains a 76 × 76 mm pocket (19 mm depth), and a circular glass window is securely mounted in the floor of the pocket. Honeycomb core can be placed into the pocket, such that the top of the



core is flush with the top of the tool plate. An interchangeable glass spacer rests on the floor of the pocket, under the core, to accommodate various core thicknesses. A 126×126 mm stack of film adhesive and prepreg is laid-up over the core, giving ~25 mm overlap onto the tool plate around each edge of the pocket, and creating a sealed “core cavity” that mimics the interior of a full sandwich assembly. Standard vacuum-bag consumables are then placed over the laminate. Various combinations of edge-breathing dams, tacky-tape-sealed edges, and perforated or non-perforated release films can be used to impose desired boundary conditions for air evacuation (i.e. transverse only, in-plane only, or both). The tool plate contains three holes near the corners, and sealant tape for the vacuum bag is applied such that one of these holes is inside the perimeter of the bag and the other two are outside. The inner hole leads to a quick-release fitting on the bottom of the tool, through which the bag vacuum is pulled (removing the need for the standard, bulky vacuum hose connector used in most vacuum bag assemblies). The outer two holes in the tool plate are used for a compressed air connection and for an interchangeable, pressure-proof thermocouple pass-through. To support super-ambient autoclave pressures (up to 7 bar), an aluminum lid is bolted over the tool plate, with an O-ring providing an airtight seal.

The co-cure fixture allows three pressures to be controlled, and four to be measured. Autoclave and vacuum bag pressures are supplied by an air compressor and a vacuum pump (respectively), controlled by manual regulators, and measured using pressure transducers. Additionally, the core cavity contains ports for a pressure transducer that measures gas pressure in the core and for a vent that allows the core pressure to be regulated, if desired. The core vent uses a quick-release fitting that creates an airtight seal when disconnected. Finally, a fourth pressure sensor is embedded in the tool plate adjacent to the core pocket. The sensor tip is recessed from the plane of the tool plate, such that prepreg fibers do not contact the sensor. During processing, once elevated temperatures cause



resin to flow and contact the sensor tip, the resin pressure in the prepreg can be measured (and compared to the applied autoclave pressure, etc.).

Two independent PID controllers (Watlow PM6R1CA) are used for temperature control. Heating elements and an embedded thermocouple in the main tool plate form the first temperature control loop, and a second, similar configuration is built into the lid. Typically, both controllers are set to the same temperature cycle, but different set-points can be imposed (e.g. to study the effects of spatial thermal gradients). Once the lid is bolted onto the tool plate, the entire assembly is wrapped in a silicone-coated fiberglass fabric for thermal insulation. The interchangeable thermocouple pass-through allows for a desired number of temperature channels to be measured within the autoclave cavity. Thermocouple tips can be placed anywhere around the vacuum bag, or even embedded within the laminate.

Visual data is recorded during testing using a portable digital microscope (Dino-Lite Edge AM7815MZTL). The microscope is aimed upwards at the window in the bottom of the core cavity, with a distance of 25 to 75 mm resulting in a field-of-view covering 5 – 20 honeycomb cells (each nominally 3.2 mm in diameter). Images are recorded at 30-second intervals and later processed into time-lapse videos. The head-on view provided by this scheme – in which we look directly along the axis of the honeycomb cells – provides visualization of bubbles/voids at the bond-line and qualitative information about fillet formation, but it is difficult to determine how far along the cell walls the adhesive moves. To address this issue, an optional alternative configuration can be used, which involves removing a square section from the honeycomb core and inserting a glass “mirror cube” (see Figure 3). This cube consists of two right-triangular prisms, bonded at their hypotenuses to form a cube, with reflective surface coatings on the hypotenuses such that light entering normal to a cube-face is rotated 90 degrees. By placing the cube into the square hole cut into the core, with the proper



orientation, the microscope's perspective is rotated from vertically-upwards to horizontal. The position of the microscope is adjusted such that half of the field of view is the side-view through the cube while the other half is directly upwards, resulting in a split field of view that enables simultaneous observation of the same fillets from two perpendicular perspectives.

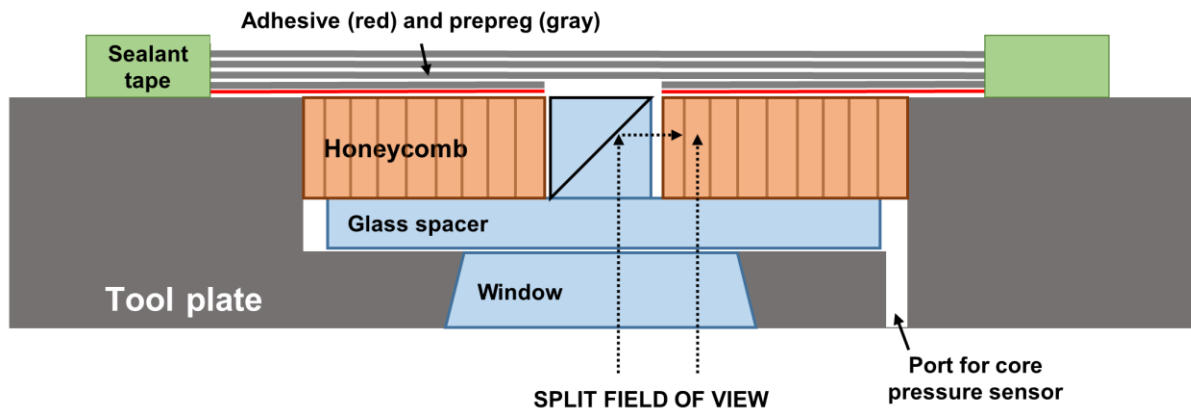


Figure 3: Schematic of the optional side-view visualization configuration (not to scale)

A digital data acquisition system (National Instruments cDAQ-9174) records the four pressure transducer outputs and up to sixteen thermocouple channels. A custom LabVIEW control panel on a desktop PC is used to monitor sensor outputs in real time and to save recorded data. The same PC controls the digital microscope and saves the captured images, which can later be correlated to the temperature and pressure data measured at the time each image was taken.

The co-cure fixture is mounted to a frame constructed from T-slotted aluminum extrusions, which also contains an enclosure that houses the power distribution for the heaters and related system components. The system fits on a countertop, and can be lifted easily by two people. The frame is designed such that the entire tool can be flipped upside down, to study the effect of the direction of gravity on fillet formation and resin bleed (i.e. to simulate the difference between tool-side and bag-side skins).



4. EXPERIMENTAL METHODS

Tests conducted using the *in situ* co-cure fixture are grouped into three types: air evacuation experiments, controlled-pressure experiments, and realistic co-cure experiments. The first type of test involves measuring the time-dependent changes in core pressure caused by evacuating the vacuum bag, to determine the air permeability of the prepreg skin. The controlled-pressure tests consist of co-curing samples under isobaric conditions, where the bag, core, and autoclave pressures are all regulated to desired values. These tests allow material behavior (e.g. volatile release, resin flow, etc.) to be characterized in controlled conditions. The final type of test – “realistic” co-cure – consists of curing samples under representative autoclave conditions. For these tests, the core pressure is allowed to naturally evolve due to the competing effects of air evacuation (which tends to reduce the core pressure) and moisture desorption from the cell walls upon heating (which, along with ideal gas law behavior, tends to increase the core pressure).

Air evacuation experiments were performed with both types of prepreg (8552S and 5320-1), using four plies in a $[(0^\circ/90^\circ)]_{2s}$ layup and without film adhesive. The purpose of this type of test is to provide experimental data with which to build a model for prepreg air permeability (which will ultimately be a key component for an integrated co-cure model). The flow of gas is required to measure permeability, therefore in these experiments, once the core pressure had equilibrated with the bag vacuum (i.e. gas flow had effectively ceased), air was re-introduced into the core pocket through the core-vent so that additional data could be collected. Although these experiments will later be conducted during temperature and pressure cycles representative of autoclave processing, the initial tests discussed here were only for room-temperature vacuum holds and under constant autoclave pressures of 101 kPa (ambient pressure) and 377 kPa (absolute, equivalent to 40 psi gauge pressure). The edges of the laminates were sealed with tacky-tape and a perforated release film was

Please cite this article as: Mark Anders, Daniel Zebrine, Timotei Centea, and Steven Nutt, “*In Situ* Observations and Pressure Measurements for Autoclave Co-Cure of Honeycomb Core Sandwich Structures”, Journal of Manufacturing Science and Engineering, 139(11), 111012 (2017). DOI: 10.1115/1.4037432



placed on top, to impose through-thickness air evacuation only. To start each test, full vacuum was applied to the bag, and the reduction in core pressure over time was recorded. Once the core pressure fell within ~ 3 kPa of the bag pressure, or ~ 1 hour had passed (whichever came first), the core cavity was manually vented to ambient pressure, and the procedure was repeated. For each vent/evacuate pressure cycle, the data was fit to a decaying exponential function, from which values for the transverse air permeability were extracted. Because this method assumed a fixed volume for the core cavity, avoiding leaks was critical. Prior to performing air evacuation experiments, the airtightness of the fixture was tested by sealing an air-impermeable metal plate over the core pocket, evacuating the core cavity (using the core vent), and measuring the changes in core cavity pressure after the vacuum hose was disconnected. The threaded fittings were tightened between measurements until, at both room temperature and the nominal cure temperature (177°C), the leak rate was < 0.1 kPa per hour.

Controlled-pressure experiments were conducted using 8552S prepreg and 9658 AERO adhesive. Layups were identical to the air evacuation experiments, except one layer of film adhesive was included between the core and prepreg. Samples were cured using a standard temperature cycle: 1 hour at 110°C , then 2 hours at 177°C , with $2^\circ\text{C}/\text{min}$ ramps. Autoclave pressure was set to 101, 276, or 377 kPa absolute (0, 20, or 40 psig), and the vacuum bag pressure was set to ~ 0 kPa (full vacuum), ~ 50 kPa (half vacuum), or 101 kPa (vented to ambient pressure). Additionally, the core vent was connected to the same vacuum line, resulting in equal pressures in the vacuum bag and core cavity throughout all tests of this type.

Finally, realistic co-cure experiments were also demonstrated. These tests followed procedures identical to the previous type, except that the core vent was left sealed shut, allowing the core pressure to evolve naturally during the cure cycle (to mimic a realistic autoclave co-cure situation).



5. RESULTS

Select results for each test category are presented here, to highlight the usefulness and versatility of the *in situ* co-cure fixture. Comprehensive analysis of a full test matrix for each category is beyond the scope of this paper, and will be the topic of subsequent publications.

5.1. Air Evacuation Experiments

Figure 4 shows measured core pressure data for 5320-1 prepreg at room temperature, with full vacuum on the bag and vacuum-bag-only compaction (no autoclave pressure). Splitting the data into individual sub-tests and resetting the elapsed time at each core-venting event results in the 16 curves shown in Figure 5.

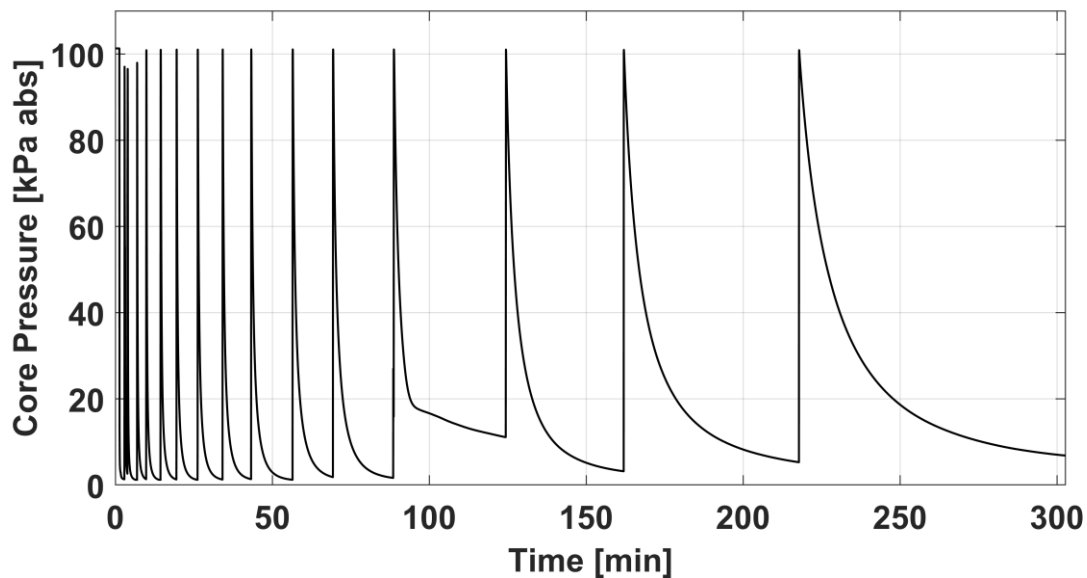


Figure 4: Falling core pressure data for an air evacuation test with 5320-1 prepreg and ambient compaction pressure

The prepreg air permeability K is a parameter in Darcy's Law (Eq. 1) [9], which describes the flow velocity v of a fluid (air in this case) with viscosity μ , through a porous medium, due to a pressure gradient. K is direction-dependent, and is thus a second order tensor (Eq. 2).

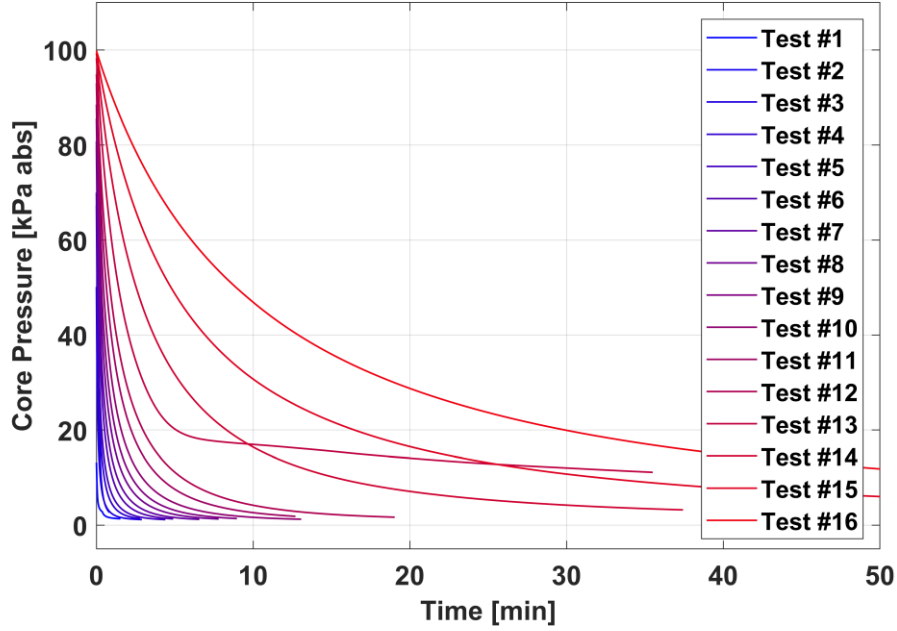


Figure 5: Falling core pressure data split into individual subtests

$$\bar{v} = -\frac{\bar{K}}{\mu} \nabla \bar{P} \quad (1)$$

$$\bar{K} = \begin{bmatrix} K_{xx} & K_{xy} & K_{xz} \\ K_{yx} & K_{yy} & K_{yz} \\ K_{zx} & K_{zy} & K_{zz} \end{bmatrix} \quad (2)$$

The experimental setup described here, with edges of the prepreg sealed, gives a measurement of transverse permeability K_{zz} only. If we assume a 1-D situation where air flows only through-thickness and impose the pressure boundary conditions at the top and bottom of the laminate ($P(t, z=0) = P_{core}(t)$ and $P(t, z=L) = P_{bag}$), an approximate linearized solution can be written. Using the procedure from Kratz et al. [9] and rearranging to solve for K_{zz} gives the following expression:

$$K_{zz}(t) = -\frac{1}{t} \frac{L\mu V_{core}}{AP_{bag}} \ln \left(\frac{(P_{core}(t_0) + P_{bag})(P_{core}(t) - P_{bag})}{(P_{core}(t_0) - P_{bag})(P_{core}(t) + P_{bag})} \right) \quad (3)$$

The right-hand side of Eq. 3 contains constant scaling factors (given in Table 1) and pressure values measured at time t and the initial time t_0 . This expression can be used to compute the



transverse air permeability K_{zz} at time t , given the change in core pressure from $P_{core}(t_0)$ to $P_{core}(t)$. Because Eq. 3 is the result of a linearization approximation, it is only valid for "small" changes in core pressure (relative to the mean pressure) [3]. Therefore, instead of using the beginning of each evacuation cycle as t_0 , a 15-second moving interval was used to compute K_{zz} (i.e. for each evaluation of $K_{zz}(t)$, t_0 was taken as $(t - 15 \text{ s})$). The permeability values computed from the data in Figure 5 are shown in Figure 6.

Table 1: Parameters used in Eq. 3

Name	Units	Value	Description
K_{zz}	m^2	[computed]	Transverse air permeability
t	s	[measured]	Time
L	m	$1\text{e-}3$	Travel length (skin thickness)
μ	$\text{Pa}\cdot\text{s}$	$1.85\text{e-}5$	Air viscosity
V_{core}	m^3	$1.1061\text{e-}4$	Core volume
A	m^2	$5.806\text{e-}3$	In-plane area
P_{core}	Pa	[measured]	Core pressure
P_{bag}	Pa	[measured]	Vacuum bag pressure

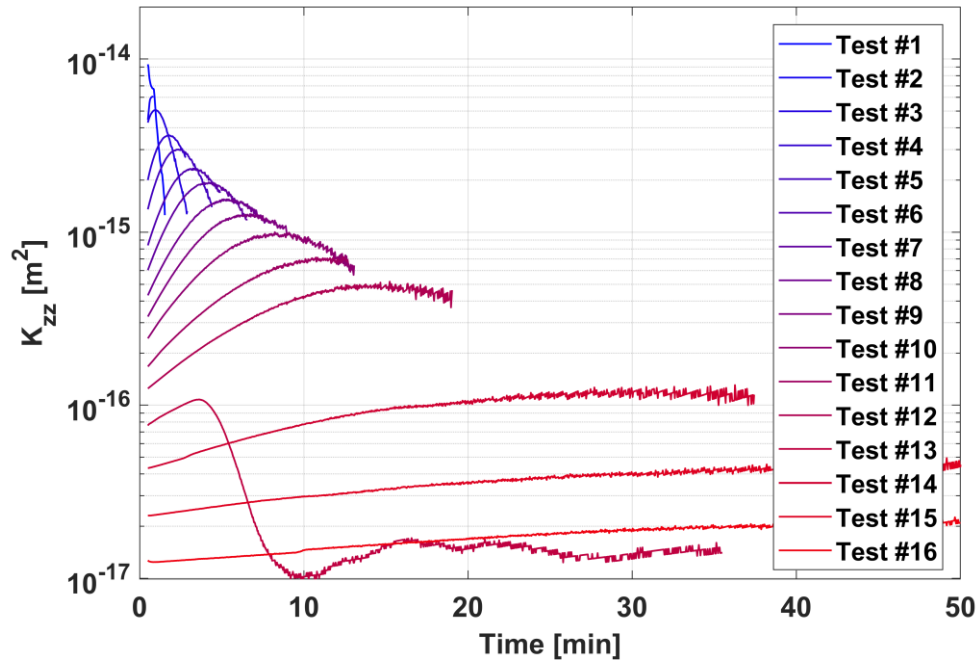


Figure 6: Transverse permeability computed from an air evacuation test with 5320-1 prepreg and ambient compaction pressure



Several trends are apparent in the data. First, K_{zz} was not constant, instead spanning several orders of magnitude. Although initial air evacuation was rapid, giving permeability values $> 10^{-15} \text{ m}^2$, the permeability decreased with each subsequent test until stabilizing near 10^{-17} m^2 . Furthermore, within each test, the permeability tended to vary. These deviations from constant- K exponential decay suggest that the gas flow through the laminate may not be solely Darcian. Kratz et al. [9] proposed the explanation that, rather than acting as a homogeneous permeable material, the prepreg skin contains discrete channels for airflow, which can form if voids through the thickness of the skin become interconnected.

The gas pressure within such a channel can influence the size and shape of the channel itself, and the widening or narrowing of the channel due to gradual flow of the highly-viscous resin could occur in a transient manner. Furthermore, the evolution of laminate thickness was not incorporated in the calculation of K_{zz} , which may introduce additional error.

The overall trend, of decreasing permeability over successive tests, is likely a consequence of plies nesting and resin cold-flowing over the cumulative time spent under compaction. The rapid pressure “shock” that the skin experiences when the evacuated core cavity is vented could cause the plies to shift, which may enhance ply nesting and contribute to the permeability decrease observed between successive vent/evacuate pressure cycles.

It may be possible to reduce these venting-induced disturbances to the state of the prepreg by limiting the pressure to which the core cavity is vented (i.e. venting not to atmospheric pressure, but from an air reservoir held at partial vacuum). However, any scheme that involves intermittent introduction of new air into the core cavity will produce successive measurements of transient behavior. Using this approach, it is difficult to determine the dependence of the effective permeability on mass flow rate, pressure differential, and total time under compaction, because all



three parameters change simultaneously during testing. An alternative procedure that will be explored in the near future consists of measuring the pressure drop across the prepreg skin for a known, steady-state rate of airflow. A mass flow controller will be connected to the core vent to introduce air into the core cavity at a controlled rate. Vacuum bag pressure will also be controlled, and the resulting steady-state core pressure can then be used to compute the permeability. Advantages of this method are: (1) all parameters (other than time) can be held at constant values, and (2) mass flow rate, compaction pressure ($P_{auto} - P_{bag}$), and driving pressure ($P_{core} - P_{bag}$) can all be varied independently. Separating the influences of these parameters will be essential to developing a rigorous model for prepreg air permeability.

The effect of autoclave pressure on prepreg permeability (at room temperature) has also been studied in preliminary tests. Figure 7 shows core pressure data for a test identical to that of Figure 4, except that the autoclave pressure was increased from ambient (101 kPa) to 377 kPa (40 psig) partway through the first evacuation cycle. Subsequent evacuation cycles slowed significantly, until after ~5 hours the prepreg stack became effectively impermeable. Figure 8 shows a comparison of the permeability values between the two experiments, plotted against the total elapsed time.

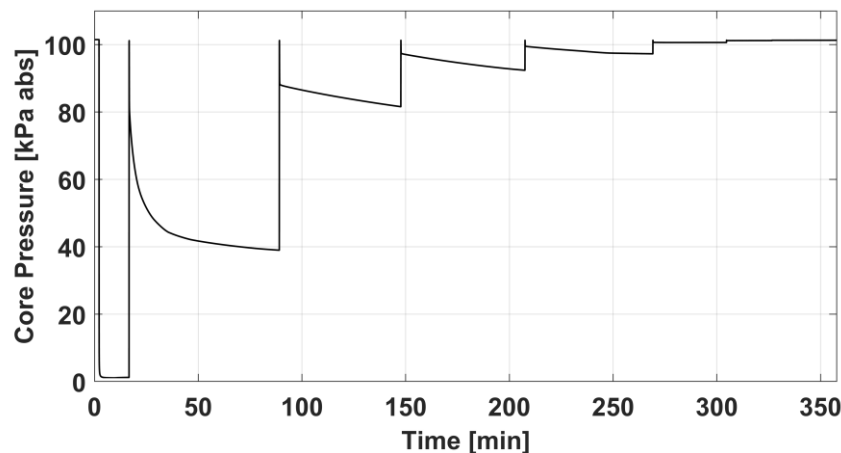


Figure 7: Falling core pressure data for an air evacuation test with 5320-1 prepreg and elevated compaction pressure

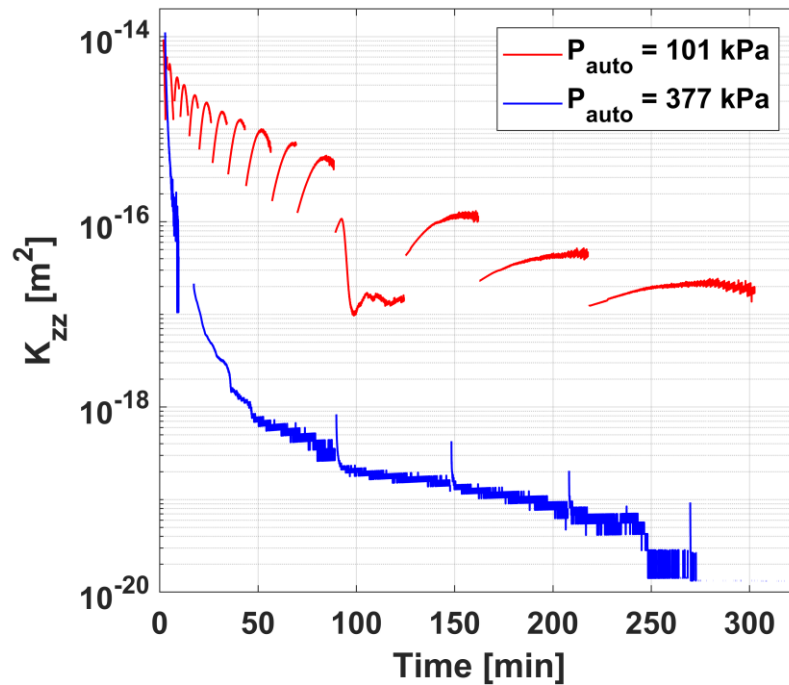


Figure 8: Transverse air permeability for 5320-1 prepreg at room temperature and two autoclave pressures

The overall trend for both samples in Figure 8 is downward with total time, but increased compaction pressure reduced the permeability further, until, after the last venting of the core, no further pressure changes were observed. Both samples exhibited fluctuations in the computed K values each time air was reintroduced through the core vent, reinforcing the need for a “steady-state” experimental procedure.

The effect of initial impregnation state has been observed, through comparable tests (not shown here, for brevity) with the second type of prepreg, 8552S. While the 5320-1 is partially impregnated (with dry fiber tows to facilitate air evacuation), the 8552S is fully impregnated. Both prepreg types have similar fabric architecture, so the primary difference between them affecting air permeability is the resin distribution. With autoclave pressure set to ambient and full vacuum on the bag, the 8552S permeability was marginally lower than that of the 5320-1, but with high variability, and



occasionally becoming spontaneously impermeable. During an overnight vacuum hold for an 8552S laminate that had become impermeable after repeated core-venting cycles, on two occasions hours apart, the laminate became briefly permeable, then impermeable again. For a sample with 377 kPa of autoclave pressure, permeability dropped to zero before the core could ever be fully evacuated.

Note that a stack of plies that is impermeable at room temperature could become permeable upon heating, since the viscosity of the resin is one of the main factors restricting airflow through the skin. The viscosity that appears in Darcy's Law in our context pertains to air, but a model for the prepreg permeability will need to include dependence on the resin viscosity and prepreg impregnation level. Future plans for these experiments include tests at higher temperatures and throughout representative cure cycles, which will provide data for developing a model that considers all relevant process parameters. Finally, note that the tests described here had sealed edges on the prepreg skins, imposing transverse air evacuation only. This can be considered representative of a small region near the middle of a larger part (far from any breathing edges). Future tests will also consider in-plane prepreg permeability by replacing the sealed edges with breathable dams (and optionally replacing the perforated release film with an air-impermeable film).

5.2. Controlled Pressure Experiments

Figure 9 shows measured temperature data for a controlled-pressure test with four plies of 8552S prepreg and one layer of 9658 AERO adhesive. Modeled properties (viscosity and glass-transition temperature T_g , from previously developed models [12,13]) are shown as dashed lines, and four times of interest are indicated by dotted vertical lines. The sample was cured under isobaric conditions: 276 kPa (20 psig) of autoclave pressure, and atmospheric pressure in both the vacuum bag and the core cavity (equal core and bag pressures were imposed for these tests to prevent continuous air flow through the prepreg stack).

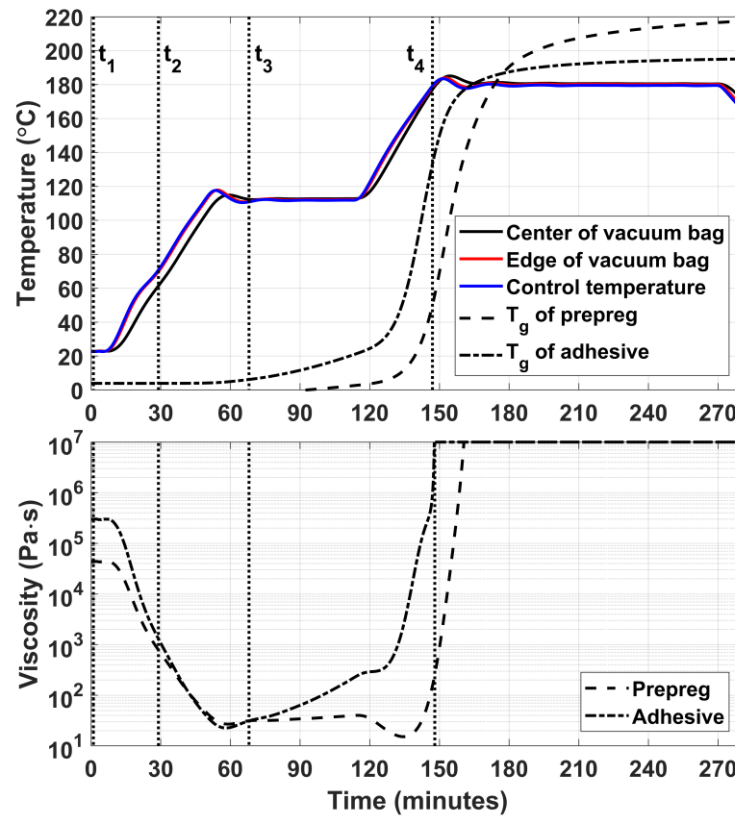


Figure 9: Measured temperatures (solid lines) and modeled material properties (dashed lines) for a controlled pressure experiment

The times of interest indicated on Figure 9 correspond to images taken by the microscope, shown in the left column of Figure 10. The right column shows images for another sample, cured using the same temperature cycle and autoclave pressure, but with full vacuum applied to both the vacuum bag and core cavity. The rows in Figure 10, top to bottom, correspond to the times t_1 through t_4 in Figure 9. For the sample cured at ambient pressure, adhesive flow began early in the first temperature ramp, and fillets had already partially formed at t_2 . Some bubbles were visible within the resin film, which likely stemmed from air that was initially trapped between the adhesive and the first prepreg ply during layup. As the fillets continued to advance down the cell walls (recall that the field of view is facing upwards), the prepreg behind the adhesive layer began to show through, and more bubbles slowly appeared. Little change was observed from t_3 until the end of the first temperature dwell, but



upon heating toward the second dwell, the bubbles roughly doubled in size and “inflated” the fillets. At this time (t_4), the onset of adhesive gelation prevented further void evolution, and no other changes were observed during the cure cycle.

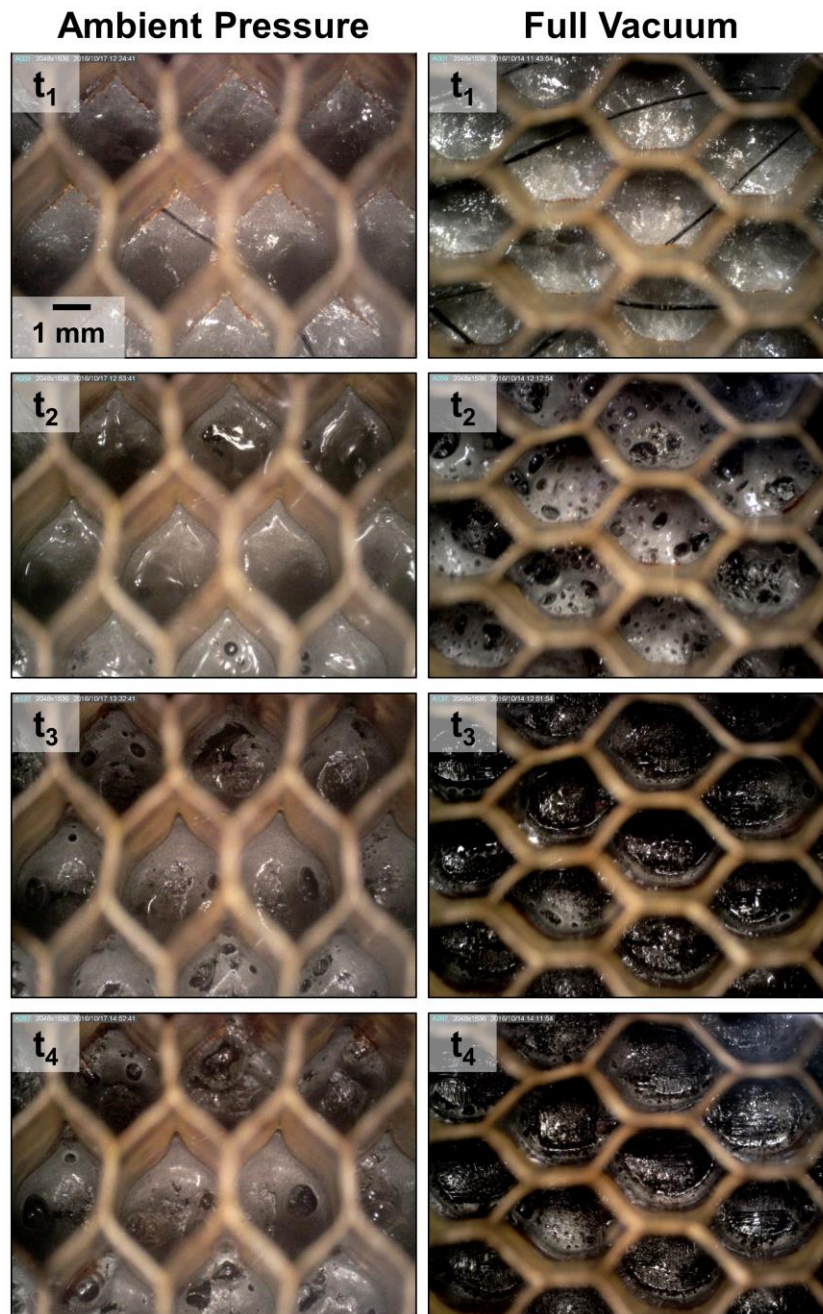


Figure 10: In situ images of bond-line formation during controlled pressure tests. Left column: ambient core/bag pressure. Right column: full vacuum on the core and bag. Times t_1 – t_4 correspond to those from Figure 9.

Please cite this article as: Mark Anders, Daniel Zebrine, Timotei Centea, and Steven Nutt, “*In Situ Observations and Pressure Measurements for Autoclave Co-Cure of Honeycomb Core Sandwich Structures*”, Journal of Manufacturing Science and Engineering, 139(11), 111012 (2017). DOI: 10.1115/1.4037432



Curing an equivalent sample under full vacuum, shown in the right column of Figure 10, resulted in markedly different behavior. In contrast to the gradual flow that was observed during the first temperature ramp at ambient pressure (driven primarily by surface tension and capillary wicking), full vacuum caused the bond-line to “froth” with rapid bubble growth and collapse (see t_2). These gas bubbles stem, in part, from volatiles released by the resin and/or adhesive (e.g. the 8552S prepreg is fabricated in a solvated tower process, and may contain residual solvent). However, the bubbles can also stem from air trapped between the plies during layup, which migrates towards the skin/core boundary due to the low core pressure. Once the first temperature dwell was reached (t_3), bubble formation effectively ceased, and most of the larger bubbles ruptured. During the remainder of the cure cycle, even during the second temperature ramp, little change was observed.

Comparison of the material behavior under these two conditions provides insight into the relationship between core pressure and fillet geometry. The fillets formed at atmospheric pressure appeared larger, but also contained large voids. Conversely, the fillets formed under vacuum were smaller but contained fewer voids. Although far more bubbles formed in the test with full vacuum, most had time to rupture before the adhesive gelled. Finally, by the difference in color at the middle of each cell, it is apparent that the foaming behavior under vacuum caused much of the adhesive to splash onto the cell walls. Without mechanical testing on these samples, it is not immediately obvious which of these bond-line morphologies is preferable in terms of strength.

5.3. Realistic Co-Cure Experiment

The data from a representative realistic co-cure test is shown in Figure 11. This sample consisted of the same layup as described in the previous section, and was cured using the same temperature cycle. Full vacuum was pulled on the bag and the autoclave cavity was vented to atmospheric



pressure (VBO conditions). The core vent remained sealed shut, such that the pressure in the core cavity evolved in conditions mimicking those of standard sandwich panel manufacturing.

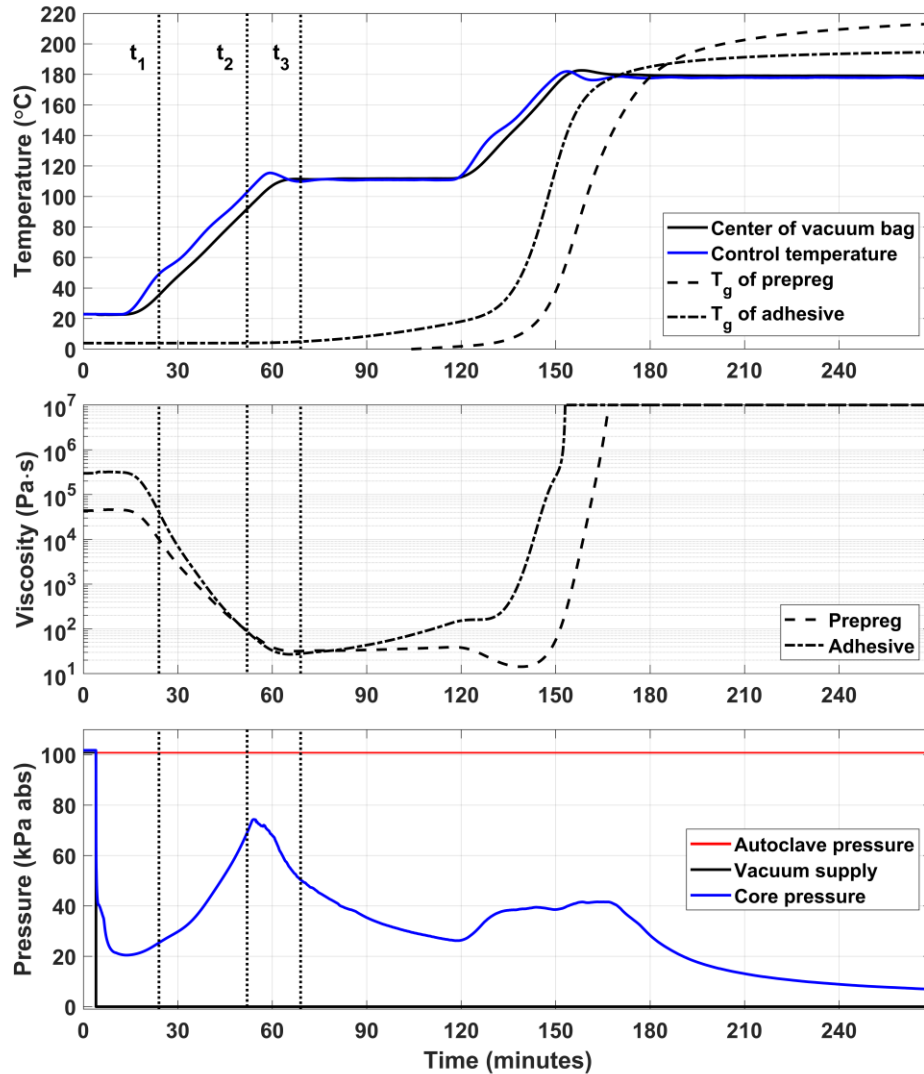


Figure 11: Data from a realistic co-cure test. Solid lines indicate measured data and dashed lines indicate modeled properties.

Upon initial application of vacuum to the bag, the core pressure rapidly dropped partway, but air evacuation slowed as the sample compacted. The first temperature ramp caused an increase in core pressure, followed by a decay during the first dwell. The second temperature ramp resulted in another, less pronounced peak, and core pressure again decayed during the second dwell.

Please cite this article as: Mark Anders, Daniel Zebrine, Timotei Centea, and Steven Nutt, “*In Situ Observations and Pressure Measurements for Autoclave Co-Cure of Honeycomb Core Sandwich Structures*”, Journal of Manufacturing Science and Engineering, 139(11), 111012 (2017). DOI: 10.1115/1.4037432

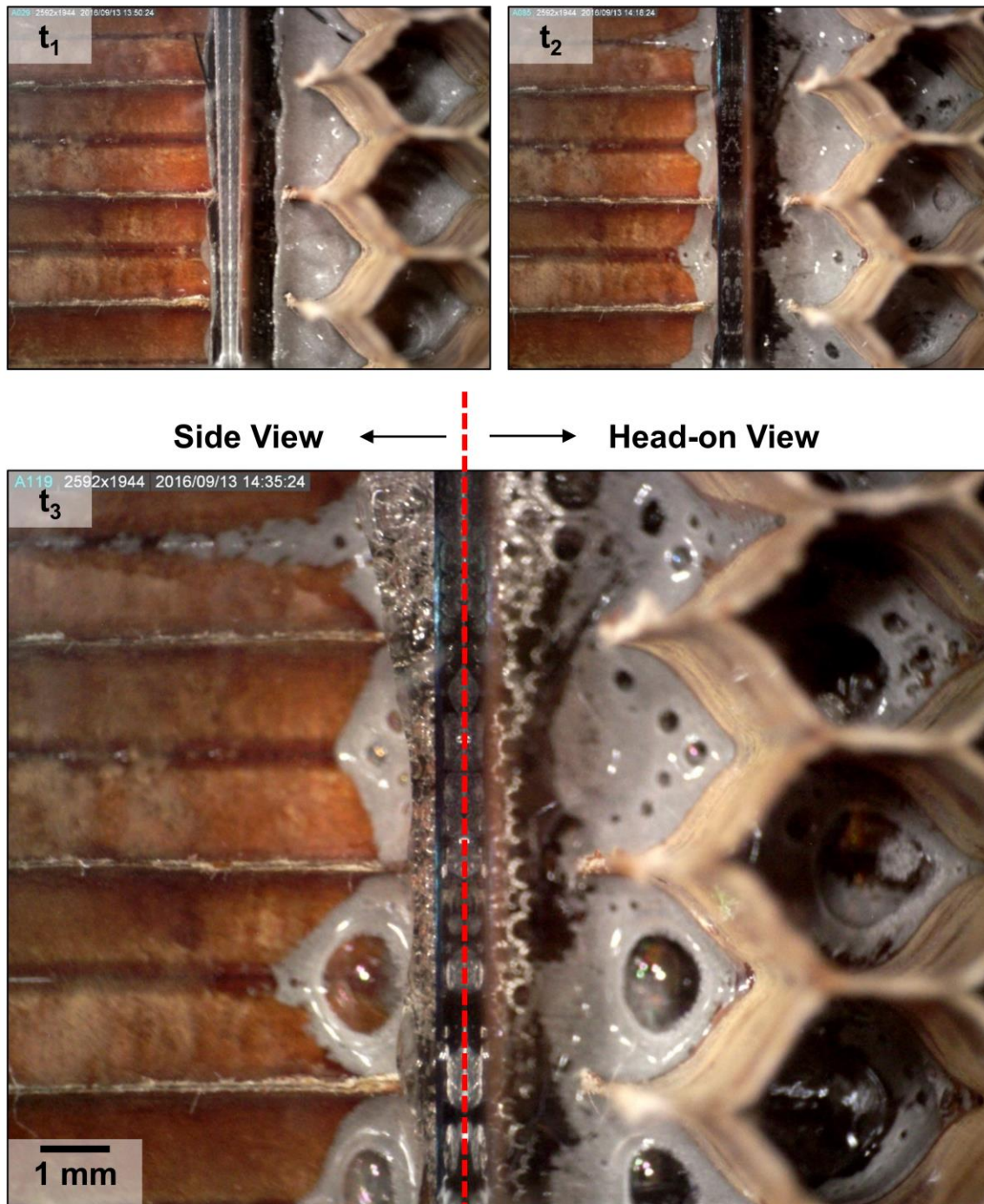


Figure 12: Images from a realistic co-cure test, taken at the times indicated on Figure 11. This test included the “mirror cube” to capture images of fillets from head-on and side-view perspectives simultaneously.

This test included the “mirror cube” that is shown schematically in Figure 3. The right half of each image in Figure 12 is the same perspective as previously, but the left half of each image contains

Please cite this article as: Mark Anders, Daniel Zebrine, Timotei Centea, and Steven Nutt, “*In Situ Observations and Pressure Measurements for Autoclave Co-Cure of Honeycomb Core Sandwich Structures*”, Journal of Manufacturing Science and Engineering, 139(11), 111012 (2017). DOI: 10.1115/1.4037432



the side-view perspective of the same cells. Early in the first temperature ramp, at time t_1 , the adhesive film had started to swell due to underlying bubbles, but remained largely intact. By the time t_2 , toward the end of the first ramp, significant adhesive flow along the cell walls had occurred (note the variability in maximum fillet height between neighboring cells), and bubbles had appeared at the surface of the adhesive. During the initial temperature overshoot (t_2 to t_3), larger bubbles formed, most of which remained until gelation. Some foaming of prepreg resin (which is clear, while the adhesive is gray) was observed during this test near the edge of the mirror cube, so its presence may have influenced the sample in unintended ways. However, there is potential benefit to conducting tests in this split-view configuration, because it enables quantitative characterization of the time-dependent fillet height.

6. CONCLUSION

The *in situ* co-cure fixture is a versatile experimental platform that enables detailed characterization of the autoclave co-cure process. This tool incorporates features from similar, previously-published permeability testing methods for VBO co-cure, but also allows autoclave pressures to be applied. Most importantly, the *in situ* visualization capability enables time-dependent process phenomena to be observed, which, to the best of the authors' knowledge, has not been published previously.

The tool and methods described herein are currently being used to construct an integrated, physics-based process model for autoclave co-cure. The model will first compute relevant properties for the constituent materials on the basis of process parameters such as temperature and pressure – for example, prepreg cure kinetics, viscosity, impregnation, and permeability; adhesive cure kinetics, viscosity, volatile release, and wetting characteristics; and moisture content of the honeycomb core.

The model will then capture the key physical phenomena and their interactions: prepreg

Please cite this article as: Mark Anders, Daniel Zebrine, Timotei Centea, and Steven Nutt, “*In Situ Observations and Pressure Measurements for Autoclave Co-Cure of Honeycomb Core Sandwich Structures*”, Journal of Manufacturing Science and Engineering, 139(11), 111012 (2017). DOI: 10.1115/1.4037432



consolidation, adhesive flow, and the gas pressure in the core. Finally, the model will output quality metrics such as final fillet geometry and the extent of porosity within the skins and adhesive.

Although prepreg air permeability measurements have been demonstrated, a comprehensive study will be required to develop a model for permeability that accounts for all relevant parameters (prepreg compaction and impregnation levels, resin viscosity, etc.). Controlled-pressure tests have shown a significant effect of core pressure on the evolution of the bond-line, but again, additional testing will be required to relate process parameter inputs, material behaviors (adhesive flow and bubbling), and the resulting part quality (porosity, peel strength, etc.). Finally, additional realistic co-cure tests will be conducted for comparison with the predictions of the physics-based process model as development continues. In all cases, the co-cure fixture and methods described in this paper will provide essential calibration and validation data.

Acknowledgement: The authors acknowledge helpful discussions with Roberto Cano, Brian Grimsley, and John Connell of NASA Langley; Suresh Advani, Pavel Simacek, and Thomas Cender of the University of Delaware; and industrial partners within the NASA Advanced Composites Project. The authors are also thankful for material donations from Cytec Solvay (Scott Lucas, Steve Howard, Chris Ridgard, Jeff Sang), Hexcel (Gordon Emmerson, Yen Wang), Henkel Aerospace Materials (David Leach), and the Gill Corporation (Jessie MacLeod).

Funding Data:

- NASA Langley Research Center (No. NRA NNL16AA13C)
- M. C. Gill Composites Center



Nomenclature:

A	area of porous medium (prepreg skin)
K	air permeability
K_{zz}	transverse (through-thickness) air permeability
L	travel length (i.e. thickness of prepreg skin)
μ	viscosity
P_{auto}	autoclave pressure (i.e. gas pressure on exterior of vacuum-bag)
P_{bag}	vacuum bag pressure (i.e. gas pressure on interior of vacuum bag)
P_{core}	core pressure (i.e. gas pressure within honeycomb core cells)
t	time
T_g	glass transition temperature
v	velocity
VBO	vacuum bag only
V_{core}	volume of gas within honeycomb core cells

References:

- [1] Campbell, F. C., 2003, *Manufacturing Processes for Advanced Composites*, Elsevier, London, Chap. 8.
- [2] Grove, S. M., Popham, E., and Miles, M. E., 2006, "An Investigation of the Skin/Core Bond in Honeycomb Sandwich Structures Using Statistical Experimentation Techniques," *Composites Part A*, 37(5), pp. 804–812.
- [3] Tavares, S. S., Michaud, V., and Manson, J.-A. E., 2009, "Through Thickness Air Permeability of Prepregs During Cure," *Composites Part A*, 40(10), pp. 1587–1596.
- [4] Tavares, S. S., Michaud, V., and Manson, J.-A. E., 2010, "Assessment of Semi-Impregnated Fabrics in Honeycomb Sandwich Structures," *Composites Part A*, 41(1), pp. 8–15.
- [5] Tavares, S. S., Caillet-Bois, N., Michaud, V., and Manson, J.-A. E., 2010, "Non-Autoclave Processing of Honeycomb Sandwich Structures: Skin Through Thickness Air Permeability During Cure," *Composites Part A*, 41(5), pp. 646–652.
- [6] Tavares, S. S., Caillet-Bois, N., Michaud, V., and Manson, J.-A. E., 2010, "Vacuum-Bag Processing of Sandwich Structures: Role of Honeycomb Pressure Level on Skin–Core Adhesion and Skin Quality," *Compos. Sci. Technol.*, 70(5), pp. 797–803.



- [7] Tavares, S. S., Roulin, Y., Michaud, V., and Manson, J.-A. E., 2011, “Hybrid Processing of Thick Skins for Honeycomb Sandwich Structures,” *Compos. Sci. Technol.*, 71(2), pp. 183–189.
- [8] Kratz, J., and Hubert, P., 2011, “Processing Out-of-Autoclave Honeycomb Structures: Internal Core Pressure Measurements,” *Composites Part A*, 42(8), pp. 1060–1065.
- [9] Kratz, J., and Hubert, P., 2013, “Anisotropic Air Permeability in Out-of-Autoclave Prepregs: Effect on Honeycomb Panel Evacuation Prior to Cure,” *Composites Part A*, 49, pp. 179–191.
- [10] Kratz, J., and Hubert, P., 2015, “Vacuum Bag Only Co-Bonding Prepreg Skins to Aramid Honeycomb Core—Part I: Model and Material Properties for Core Pressure During Processing,” *Composites Part A*, 72, pp. 228–238.
- [11] Kratz, J., and Hubert, P., 2015, “Vacuum-Bag-Only Co-Bonding Prepreg Skins to Aramid Honeycomb Core—Part II: In Situ Core Pressure Response Using Embedded Sensors,” *Composites Part A*, 72, pp. 219–227.
- [12] Centea, T., Zebrine, D., Anders, M., Elkin, C., and Nutt, S. R., 2016, “Manufacturing of Honeycomb Core Sandwich Structures: Film Adhesive Behavior Versus Cure Pressure and Temperature,” *Composites and Advanced Materials Expo (CAMX)*, Anaheim, CA, Sept. 26–29, Paper No. 0096.
- [13] Van Ee, D., and Poursartip, A., 2009, NCAMP Hexply Material Properties Database for Use With COMPRO CCA and Raven, National Center for Advanced Materials Performance (NCAMP), Wichita, KS.